

CHAPTER 17

LABORATORY GENERATION OF WAVES OF CONSTANT FORM

J. Buhr Hansen* and Ib A. Svendsen*

ABSTRACT

The paper reports measurements of waves generated by a piston type wave generator. The experiments show that for $0.10 < h/L < 0.65$ the waves produced by a sinusoidal piston motion can be described as a second order Stokes wave superimposed by a free second harmonic wave. Results are presented for the height and phase velocity of the free second harmonic wave and compared with theories by Fontanet (1961) and others. Finally, the height of the free second harmonic wave is successfully reduced by a non-sinusoidal time variation of the piston motion, whereas addition of a rotation to the flap motion appears to yield only minor improvements.

1. INTRODUCTION

The waves produced by a sinusoidal motion of a flap type wave generator do not have the ideal constant form which should be expected from the regularity of the flap motion. As the waves propagate they slowly change form in a periodic way, which depends on both the wave steepness H/L and the relative water depth h/L (H being the wave height, L the wave length, and h the undisturbed water depth, Fig. 1).

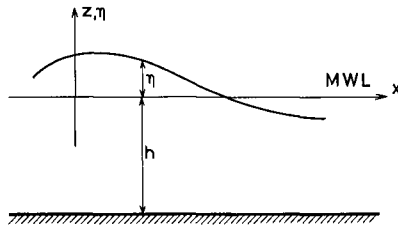


Fig. 1 Definition sketch

*Assoc. Prof., Institute of Hydrodynamics and Hydraulic Engineering (ISVA), Technical University of Denmark, DK-2800 Lyngby

Fig. 2 shows (in one of the more extreme cases) the time variation of the surface elevation at different points along a wave flume. This pattern will be familiar to most laboratory people. The reason for the irregularities is, of course, that a rigid flap cannot exactly produce the variation of the particle motion which corresponds to a progressive wave of constant form.

The first reference to this phenomenon seems to be in Biésel and Suquet (1951), whose description clearly accounted for the basic principle described above. Since then many others have given more or less conscious experimental reports of the phenomenon (see e.g. Morison and Crooke (1953), Le Méhauté et al. (1968), Iwagaki and Sakai (1970)) and several contributions have directly treated the problem analytically, numerically and in experiments (see e.g. Fontanet (1961), Goda (1967), Madsen et al. (1970), Madsen (1970), Madsen (1971), Hulsbergen (1972), Daugaard (1972), Mei and Ünlüata (1972)).

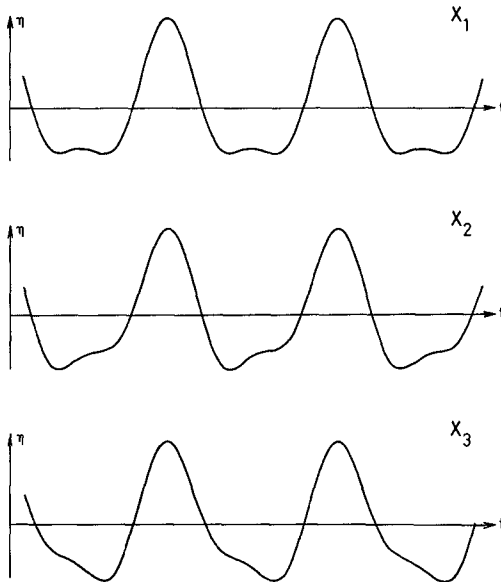


Fig. 2 Wave profile at different stations in a wave flume

An analysis of Fig. 2 suggests as a crude explanation of the motion that a smaller wave is travelling down the flume superimposed on the main wave, but with a somewhat smaller speed. Theoretical considerations show (Fontanet (1961)) that to the lowest approximation the period of this wave is $T/2$ (where T is the period of the main wave), and its height is $O(H^2)$. Accordingly this wave is denoted the 'free second harmonic wave'. [The phenomenon should not be confused with the second-

ary wave crest, which for sufficiently large wave steepness is predicted in the wave trough by the second order Stokes' theory. That is a purely theoretical effect caused by the truncation of the Stokes' theory to second order at or beyond its limit of validity.]

Hence, if we include all terms to second order the surface elevation η can be written as the superposition of a second order Stokes' wave and a free second harmonic wave, i.e.

$$\eta = a_1 \cos(\omega t - kx) + a_2 \cos 2(\omega t - kx) + a_{22} \cos(2\omega t - k_{22}x + \alpha_{22}) \quad (1-1)$$

where $\omega = 2\pi/T$ is the wave frequency and $(k, k_{22}) = 2\pi(L, L_{22})^{-1}$ the wave numbers which satisfy the dispersion relations

$$\omega^2 - g k \tanh kh = 0 \quad (1-2)$$

$$(2\omega)^2 - g k_{22} \tanh k_{22}h = 0 \quad (1-3)$$

It is important to notice that the wave pattern (1-1) apart from representing the disturbed wave profile of Fig. 2 also exhibits an apparent variation in mean water level from place to place. This can be seen if we for a moment follow a wave crest by assuming $\omega t - kx = 0$, i.e. $\omega t = kx$. Then (1-1) reads

$$\eta_{\text{crest}} = a_1 + a_2 + a_{22} \cos [(2k - k_{22})x + \alpha_{22}] \quad (1-4)$$

and a similar expression for the wave trough. Hence, except for small terms the upper and lower envelope of the wave motion will be constant in time but meander with x as shown in Fig. 3.

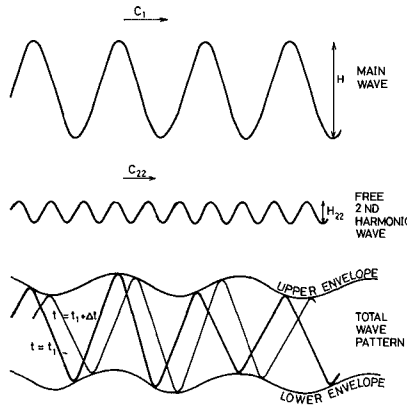


Fig. 3 Superposition of second order Stokes main wave and free second harmonic wave

As (1-4) shows the amplitude of the meander will equal the amplitude of the free second harmonic wave. Also the maxima and minima for the envelopes appear at fixed points down the wave flume, the position of which depends only on the main wave data and the phase angle α_{22} between the main wave and the free second harmonic wave at the wave generator.

It is the purpose of this paper to present some measurements of the phenomenon described above to check the model (1-1) and to report results obtained by giving the flap of the wave generator a non-sinusoidal motion, scaled to reduce the (unwanted) free second harmonic wave motion to a minimum.

During the experiments several other unwanted effects have appeared. Some of them are obviously third or higher order phenomena, others have not been understood at all. The more important of these will be discussed in Section 5, the primary concern being to ensure that they have no or only negligible influence on the measurements in question.

2. EXPERIMENTAL SET-UP

The experiments were made in a wave flume, 60 cm wide and 25 m long (Fig. 4). Waves were generated by a hydraulic flap type wave generator. The wave generator was controlled by a mini-computer (Type PDP8E) which produced an electrical signal for the instantaneous position of the flap. The computer was also used for collecting data from the measurements. Three series of experiments have been made, distinguished by the type of the wave generator flap:

- (a) Pure sinusoidal translation (piston motion), $(e \sin \omega t)$
- (b) Pure sinusoidal motion with combined translation and rotation $(e_b(1 + e_s z/(e_b h)) \sin \omega t$, e_b and e_s being flap amplitudes at the bottom and the surface)
- (c) Piston motion composed of two sines $(e \sin \omega t + e_2 \sin(2\omega t + \varphi))$

In all experiments a wave height meter was mounted on a small carriage travelling slowly along the flume (about 1 cm per wave period). Information from the wave height meter was collected, by the computer 100 times per wave period and through a determination of each maximum and minimum for the instantaneous surface elevation the series of wave heights were computed and stored in digital form.

The data were analysed simultaneously by a digital filter* which passed only the total second harmonic component of the wave motion corresponding to the second and third terms in (1-1). Here again the series of heights of the total second harmonic component were computed and stored in digital form.

During one travel of the carriage down the flume the total wave height and the height of the total second harmonic component were stored in the computer for about 500 consecutive waves, constituting one run or test.

*The authors have been informed that the digital filter used is a fourth order band-pass filter of the Chebyshev type with 2 dB ripple. The first harmonic component is damped 48 dB (~ 250 times) by the filter. Due to the design criteria for this type of filter only 20 sampled values per wave period are passed through the filter (private communication with Mr. Peter Schjolten).

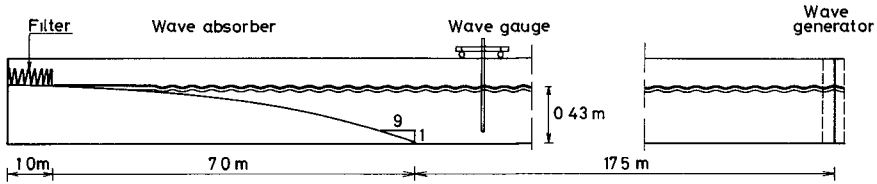


Fig. 4 Wave flume

3. EXPERIMENTAL RESULTS FOR SINUSOIDAL FLAP MOTION

These experiments comprise points (a) and (b) in the list above.

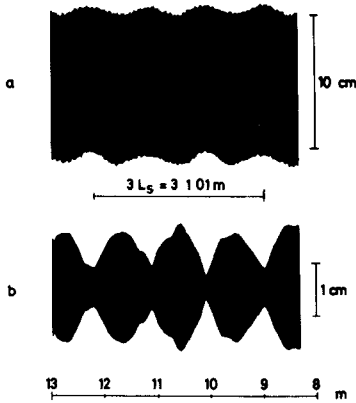


Fig. 5
Record of total wave motion
and total second harmonic motion

Fig. 5 shows an example of a record compressed to show the variation of the wave motion envelopes. Part a represents the total wave motion, part b the total second harmonic motion.

First of all the meander pattern predicted by the simple model described in the introduction is easily recognized. It is also found in each experiment to be fixed in time relative to the wave generator as (1-4) shows, the position and meander length depending only on the main wave data.

This effect is repeated in the total second harmonic component as a beat (or wave group) pattern emerging from addition of the two second order terms in (1-1). Apparently the total second harmonic component of (1-1) can also be written (neglecting the phase angle α_{22})

$$\eta^{(2)} = (a_2 - a_{22}) \cos 2(\omega t - kx) + 2 a_{22} \cos(2\omega t - \frac{2k + k_{22}}{2} x) \cos(\frac{1}{2}(k_{22} - 2k)x) \tag{3-1}$$

where the last term represents the group effect. Notice, that since

this emerges from two waves of different wave lengths but the same frequency, the group pattern is stationary in the flume.

From (3-1) (or (1-4)) we see that the theoretical distance between two maxima or two minima will be $L_{S,1}$ where

$$\frac{1}{2} (k_{22} - 2k) L_{S,1} = \pi \quad (\text{or } (2k - k_{22}) L_{S,1} = - 2\pi) \quad (3-2)$$

so that

$$L_{S,1} = \frac{L L_{22}}{L - 2L_{22}} \quad (3-3)$$

where L corresponds to k and L_{22} to k_{22} . Hence $L_{S,1}$ is also the meander wave length.

The height $H_{22} = 2 a_{22}$ of the free second harmonic wave can be found as half the difference between $H_{\max}^{(2)}$ and $H_{\min}^{(2)}$ which again can be determined with fair accuracy from part b of the figure. Thus

$$H_{22} = \frac{1}{2} (H_{\max}^{(2)} - H_{\min}^{(2)}) \quad (3-4)$$

3.1 RESULTS FOR H_{22}

The values of H_{22} measured in this way are shown in the four figures, 6 a through 6 d, representing four different wave steepnesses. The abscissa is h/L and the ordinate H_{22}/H_2 .

H_2 in the figures has been determined as

$$H_2 = \frac{1}{2} (H_{\max}^{(2)} + H_{\min}^{(2)}) \quad (3-5)$$

and these values are in Table 3-1 compared with the theoretical values determined from Stokes' theory. Some typical cases have been chosen and the agreement is not exciting, though in some cases it is remarkably good. We shall return to this point later on.

Table 3-1 Comparison of theoretical and measured values of H_2

Test No.	h cm	$\frac{h}{L}$	H mm	$\frac{H}{L}$	H_2	H_2	$\left(\frac{H_{22}}{H_2}\right)_{\text{meas}}$	$\frac{H_{22, \text{meas}}}{H_{2, \text{theor}}}$
					theor. mm	meas. mm		
2-10B	43	0.171	119.6	0.048	21.5	20.3	0.20	0.19
4-10B	30		82.5	0.047	14.6	15.5	0.27	0.29
2-10D	43		27.7	0.011	1.15	1.25	0.21	0.23
4-10D	30		19.3	0.011	0.80	0.72	0.42	0.38
2-6A	43	0.290	100.4	0.068	13.1	12.9	0.50	0.49
4-6A	30		67.1	0.065	8.37	8.32	0.35	0.35
2-6C	43		35.0	0.024	1.59	1.40	0.45	0.40
4-6C	30		24.7	0.024	1.13	0.97	0.67	0.57
2-3A	43	0.463	63.3	0.068	7.00	9.61	0.28	0.38
4-3A	30		44.4	0.069	4.90	5.16	0.27	0.28
2-3C	43		20.5	0.022	0.73	0.60	0.51	0.42
4-3C	30		14.3	0.022	0.51	0.41	0.51	0.41

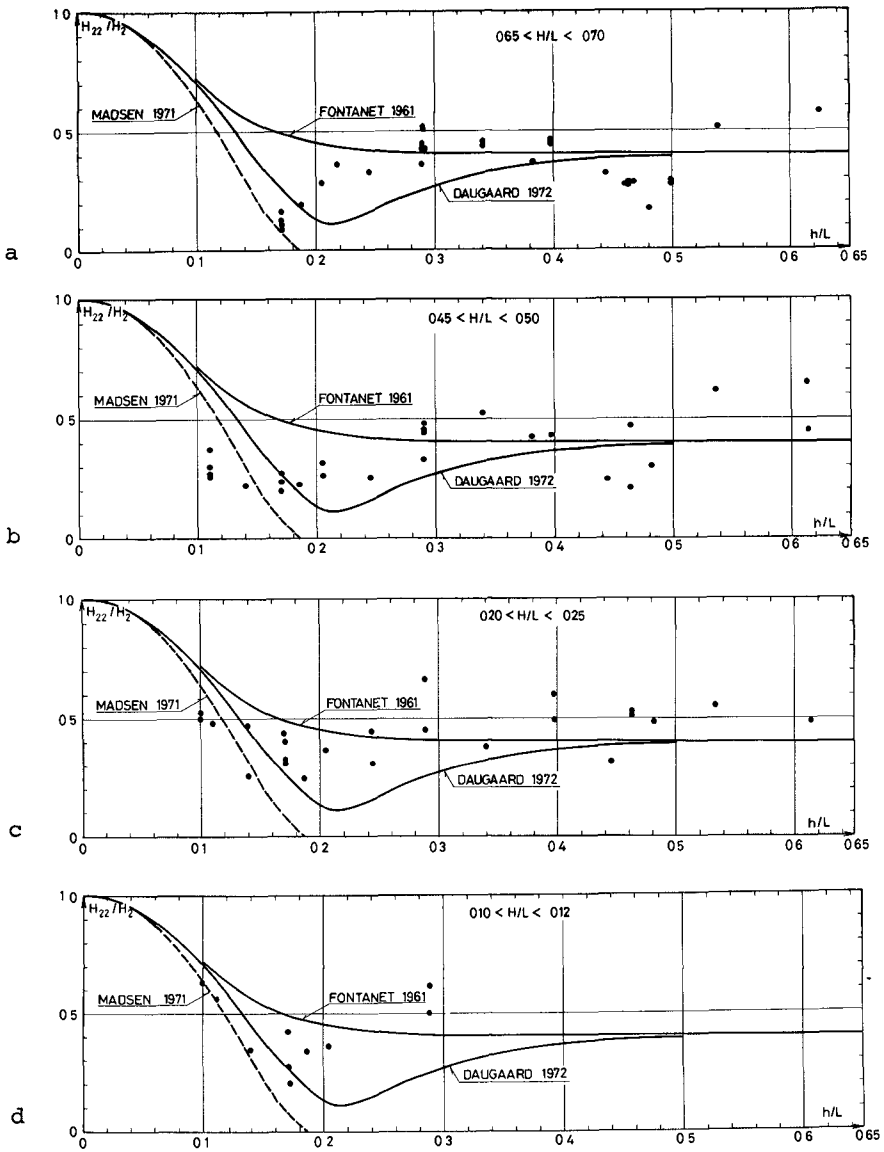


Fig. 6 Theoretical and experimental results for H_{22}

H_{22} has been determined theoretically by Fontanet (1961), his results being shown in the figures too. Also the shallow water approximation by Madsen (1971) is plotted. This theory, however, will only yield reasonable approximations for $h/L < 0.05$ (or 0.1 at most), and in that region other effects mentioned later will influence the results. Finally, the results obtained by Daugaard (1972) is shown in the Figs. 6 a through 6 d.

The experimental results in the region $0.1 < h/L < 0.65$ show two important deviations from the theoretical prediction by Fontanet.

One is a certain dependence of the results on the main wave steepness. The theory shows no such variation because it is only a second order theory. As the free second harmonic wave is of the second order, non-resonant interaction between the main wave and the free second harmonic wave will be of the third order.

The other deviation is represented by the actual variation of H_{22}/H_2 , which shows two minima, one for h/L about 0.15, the other close to $h/L = 0.45$.

The minimum at $h/L = 0.15$ is consistently found for all wave steepnesses, — even for the small waves of 1-1.25%. It is in this connection interesting to notice that although Madsen's theory is too inaccurate for $h/L > 0.1$, it does frame the experimental results around this minimum. Daugaard's theory even shows a minimum but shifted to $h/L \sim 0.22$. It should be mentioned here, that Daugaard's theory is an approximate second order theory, where some of the smallest second order terms have been omitted. It is not satisfactory but is included to emphasize, what is also indicated by the experimental results, that the failure of Fontanet's theory to predict the details of the variation of H_{22}/H_2 does not seem to be a fundamental shortcoming of a consistent second order approximation.

The other minimum has a somewhat more doubtful character. It is only recorded for the steeper waves (those of 5% and 7%), and when the records of the second harmonic component at this minimum is analysed more closely it appears that the beat effect shown in Fig. 5 b oscillates down the wave flume. The resulting range in H_{22}/H_2 corresponds to a factor of 2-2.5, of which H_2 is responsible for at least a part, as Table 3-1 shows. This probably affects the reproducibility of the experiments even for the largest waves.

Actually Table 3-1 shows results for three different values of h/L . The first group of data is for $h/L = 0.171$, corresponding to the first minimum in results for H_{22}/H_2 . The good agreement between theory and measurements of H_2 for this group of tests reflects the general impression that the model represented by (1-1) for h/L in this region gives a realistic description of the wave pattern in the flume. All the wave groups of the second harmonic signal have the same form (only the amplitude being slightly modified with increasing x due to energy dissipation).

This also applies to the second group, where $h/L = 0.29$. An exception is the last test which, however, also shows a poor agreement in Fig. 6 c with the rest of the data obtained for that wave period.

The last group of points refer to the second minimum and here the agreement is unsatisfactory. It may be worth-while to notice that the value of measured H_{22} over theoretical H_2 tends to bring the points to the value predicted theoretically by Fontanet. As mentioned above the amplitude of the group pattern oscillates with x around this value of h/L , distance between two maxima being 10-15 times L_s . No corresponding oscillation can be detected in the first harmonic component. The values in Table 3-1 are mean values and the maximum values for H_{22}/H_2 are also about 0.40.

In spite of all these uncertainties evidence presented in Section 4 seems to show that the value of $H_{2,2}/H_2$ is about 0.30 for $h/L \sim 0.45$, which means that there is a (weak) minimum there.

3.2 RESULTS FOR THE MEANDER LENGTH L_S AND PHASE VELOCITY $C_{2,2}$

The theoretical value $L_{S,1}$ of L_S determined by (3-3) is shown in Fig. 7. Since (3-3) involves only linear considerations, $L_{S,1}$ is independent of the wave steepness.

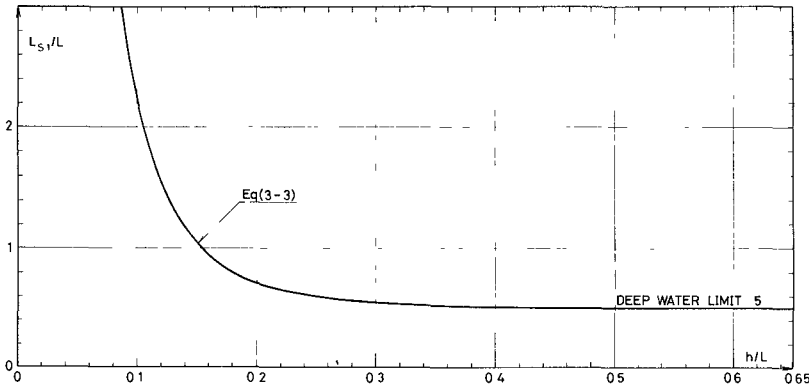


Fig. 7 Theoretical values of $L_{S,1}/L$ for the meander length

The experimental results for L_S , however, shows a quite marked variation with H/L . This is shown in Fig. 8 where the ratio $L_S/L_{S,1}$ between the experimental and the theoretical meander length has been plotted versus H/L (or kH) for 5 values of h/L . For sufficiently small values of h/L (less than about 0.11) L_S will decrease with increasing wave steepness. For $h/L \sim 0.11$, L_S is independent of H/L , and then for $h/L > 0.11$, L_S increases with H/L .

The reason for this is, of course, partly connected with the fact, that for waves of finite amplitude the phase velocity depends on the wave steepness. In Stokes wave theory this dependence is represented from the third order approximation, for cnoidal waves already in the first approximation. Since the amplitude of the main wave is always more than ten times that of the second harmonic component, it is consistent to infer that it is primarily the value of the main wave length L in (3-3) which depends on H/L .

If we introduce the third order Stokes' approximation L_3 for L by writing $c_3 = L_3/T$ but stick to the linear values for $L_{2,2}$, then (3-3) can be written

$$\frac{L_{S,3}}{L_{S,1}} = \frac{c_3}{c_1} \frac{c_1 - c_{2,2}}{c_3 - c_{2,2}} \tag{3-6}$$

where $c_1 \equiv L/T$. (Actually in the experiments where $h/L < 0.14$ a cnoidal approximation for L would be justified.) This has been utilized in

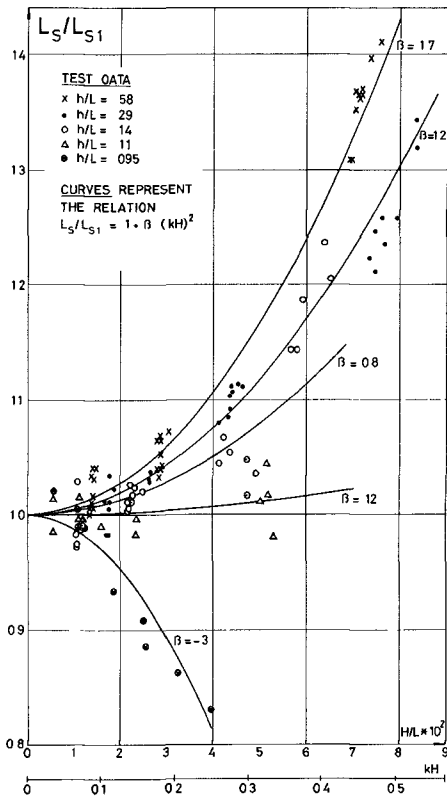


Fig. 8 Experimental results for L_s versus H/L

measurements were all in fairly shallow water ($0.05 < h/L < 0.10$) it seems unlikely from Fig. 9 that c_{22} should be so small even in that interval.

Comparing Figs. 8 and 9 it should be noticed that the value of L_s is much more sensitive to small changes in the phase velocity of the main wave than is c_{22} calculated from L_s . Hence, provided c_3 is a fair approximation to the phase velocity of the main wave, the relatively accurate measurements of L_s yield good results for c_{22} .

However, even with the third order effects included the value of c_{22} is larger than predicted by linear theory.

It turns out that there is another effect which at least in principle draws in that direction. That is caused by the net particle motion in the main wave, which represents a mean velocity U given by

$$\frac{U}{c_1 (kH)^2} = \frac{1}{8 \sinh^2 kh} \left(\cosh 2k(z+h) - \frac{\sinh 2kh}{2kh} \right) \quad (3-9)$$

Fig. 9 which shows theoretical curves for the ratio c_3/c_1 . Here c_3 given by Brink-Kjær (1974) as

$$c_3 = c_1 \left(1 + A - \frac{(kH)^2}{4 kh \tanh kh} \right)^{1/2}$$

$$A = \frac{(kH)^2 (9 + 8 \cosh^4 kh - 8 \cosh^2 kh)}{32 \sinh^4 kh} \quad (3-7)$$

corresponds to zero net mass transport (as it must be expected in a closed wave flume). The abscissa is again h/L . From the measured values of L_s has been calculated the value of c_{22} under the assumption that in (3-6) $L_{s,3} = L_s$, and that c_3 is given by (3.7). We then get

$$\frac{c_{22}}{c_3} = \frac{1}{1 + c_3 T / (2 L_s)} \quad (3-8)$$

The empirical values of c_{22} thus obtained have also been plotted in Fig. 9, and for comparison the theoretical linear curve for c_{22} is shown too.

We see that there still is a variation of the empirically determined c_{22} values which generally increase with H/L . Also the absolute values are somewhat in contradiction with Goda (1967) who reported measurements of c_{22} about 15% below the linear theoretical values. Although his

(In (3-9) has been assumed that the return flow added to yield zero mass transport is constant over the water depth. In a real wave flume this may not be true, because the downrush from the beach can cause a stronger return flow along the bottom. This has not been checked.)

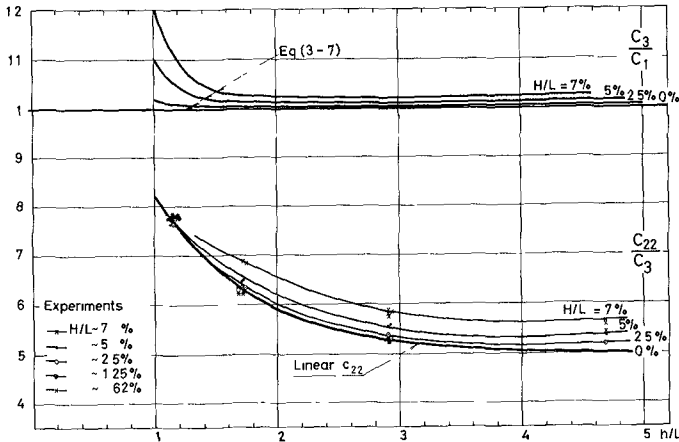


Fig. 9 Phase velocities for main wave and free second harmonic wave

In the case of deep water waves, which at least applies to the results for $h/L = 0.58$ in Fig. 8, the wave length L_{22} of the free second harmonic wave is $L/4$. Therefore, in the free second harmonic wave, the water motion is largely restricted to the upper part of the water body where the mean (or net) particle motion of the main wave will be in the direction of wave propagation as Fig. 10 shows. Retaining the assumption that the two waves, the main wave and the free second harmonic wave, do not interact, then yields a physical model, where the net particle motion of the main wave near the surface merely acts as a current carrying the free second harmonic wave with it, and thus virtually adding to the phase velocity of that wave, a contribution which is also $O(H^2)$.

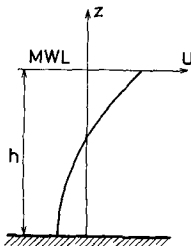


Fig. 10 Net particle velocity in second order Stokes wave with zero mass transport

The order of magnitude of this effect can be obtained from (3-9) as U at the surface (it must actually be somewhat less, say 70%). From (3-9) we get at $z = 0$ (and thus neglecting higher order effects)

$$\frac{U_s}{c(kH)^2} = \frac{1}{8 \sinh^2 kh} + \frac{1}{4} - \frac{\coth kh}{8 kh} \tag{3-10}$$

which has been confirmed to within 10 - 15% by actual measurements.

It appears (as an example) that for $h/L = 0.62$ and $H/L = 7\%$ the full effect of U_s on c_{22} will change c_{22}/c_{13} in Fig. 9 from 0.565 to 0.52 against the theoretical value of 0.50. Thus the effect of the net particle velocity seems at least to be of the right order of magnitude.

3.3 THE EFFECT OF INCLUDING ROTATION IN THE MOTION OF THE WAVE GENERATOR

As mentioned in the introduction, the free second harmonic wave appears because the water motion induced by the rigid flap does not correspond exactly to motion in a progressive wave of constant form.

In particular for increasing h/L the piston motion becomes a poor approximation. Hence it is natural to investigate, to which extend the height of the free second harmonic wave can be reduced by letting the motion of the wave generator be a combination of a translation and a rotation, the time variation remaining sinusoidal.

In Fig. 11 are shown results for H_{22}/H_2 when the motion of the wave generator varied from zero motion at the bottom ($e_p/e_s = 0$) to pure translation ($e_p/e_s = 1$), e_p and e_s being flap amplitudes at the bottom and the surface, respectively.

The general impression is that the free second harmonic motion can be reduced by this measure but not to a level, which makes the results acceptable. In particular in the third case, corresponding to deep water, one would have expected a much more pronounced effect from a rotation of the flap.

The two first parts of the figure shows a minimum for H_{22}/H_2 for all wave

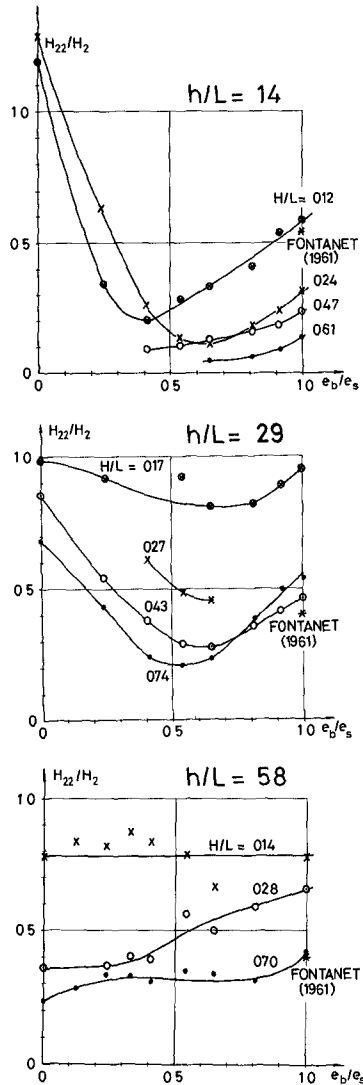


Fig. 11 Variation of H_{22}/H_2 with rotation of flap

steepnesses. The corresponding optimum value of e_b/e_s , however, is much smaller than would be expected from an estimate based on linear wave theory.

Since the effect of rotation is so relatively small we shall not go further into the various curiosities of the results.

4. GENERATION OF WAVES OF CONSTANT FORM
BY A NON-SINUSOIDAL FLAP MOTION

The third series of tests (type (c) mentioned above) aimed at reducing the free second harmonic motion by introducing a compensation for this motion of the same frequency 2ω but in antiphase.

Thus the flap motion ξ in question is a pure translation with the time variation

$$\xi = e_1 \sin \omega t + e_{22} \sin(2\omega t + \beta_{22}) \tag{4-1}$$

where β_{22} is the phase angle between the two components of the flap motion.

These experiments could have been based on the results reported in Section 3.2 for H_{22} , together with information on the phase angles α_{22} for the free second harmonic waves produced there. However, having not been able to measure α_{22} with sufficient accuracy the experiments were instead of optimized to yield minimum H_{22}/H_2 . In this way values are obtained for e_{22} and α_{22} which can be converted — by means of the linear wave generator theory (Biésel and Suquet (1951)) — to a total secondary wave height, from which a H'_{22} is determined.

Hence the value of H_{22} emerging from this series of tests serve not only as a check on the idea of reducing the unwanted secondary wave motion by a more complicated time variation of the flap motion. It can also be used as a control on the measurements of H_{22} reported in Section 3.

Figs. 12 and 13 show results for H'_{22} and α'_{22} the imaginary free second harmonic motion generated by the last term in (4-1) in antiphase to the anticipated free second harmonic motion in order to quench the latter.

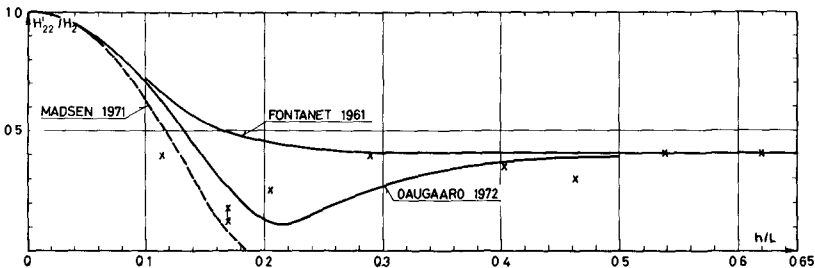


Fig. 12 Values of H'_{22}/H_2 corresponding to optimal choice of e_{22} in (4-1)

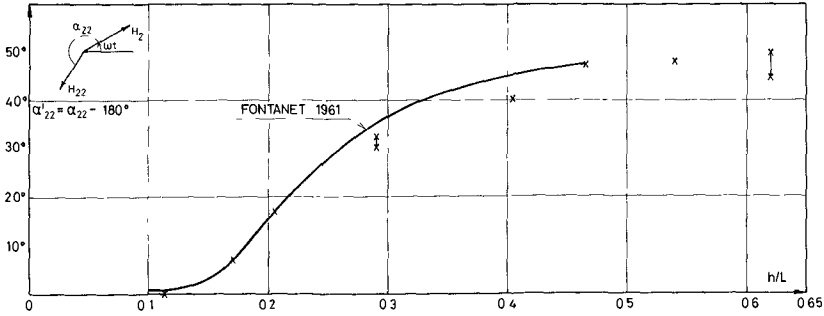


Fig. 13 Values of α'_{22} corresponding to optimal choice of β_{22} in (4-1)

Of particular interest is the confirmation of the two minima at $h/L = 0.15$ and 0.45 .

Also the different nature of the minima are confirmed. Around $h/L = 0.15$ an e_{22} value determined according to the Fontanet theory will yield a free second harmonic motion as large as or larger than that of pure sine flap motion. At $h/L = 0.45$ the value of H_{22} can be reduced to 8% of H_2 by the optimal flap motion ($H'_{22}/H_2 = 0.30$), but an $H'_{22}/H_2 = 0.40$ as suggested by Fontanet's theory will yield an actual H_{22} which is only 16% of H_2 .

In Fig. 14 is shown the values achieved for the free second harmonic motion by the optimal choice of e_{22} and β_{22} in (4-1). Since the flap still does not follow the ideal particle motion of a purely progressive wave, there must still be some free second harmonic motion left. On the other hand, even for the steepest waves H_2 is only a fraction of H and hence the disturbance is in most cases reduced to 1 or 2% of the main wave height.

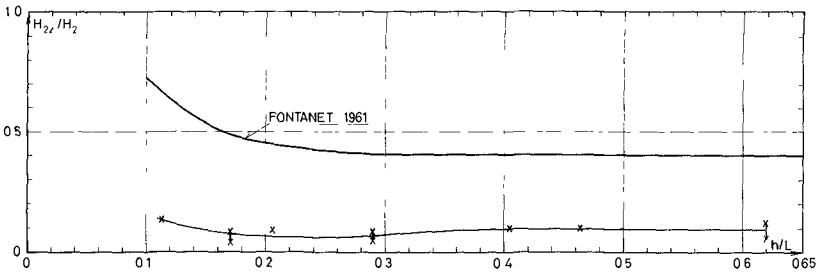


Fig. 14 Values of H_{22} with flap motion according to (4-1)

This conclusion does not apply to the region $h/L < 0.1$, i.e. long waves. For such waves Stokes' theory yields poor results as soon as the waves have any appreciable height, and really good results cannot be expected for a flap motion like (4-1). Instead a cnoidal time variation of the flap should be used, and no attempts have been made in that direction so far.

In Fig. 15 is shown a record of the wave motion in the flume with $T=1.0$ s, $H=11$ cm, $h=43$ cm, i.e. the same wave as in Fig. 5. H_{22}/H_2 is in Fig. 15 reduced to 0.10 by the non-sinusoidal flap motion, resulting in an almost constant second harmonic component. (Instead a second order reflection becomes clearly visible. This problem is discussed in more detail in Section 5.) The overall impression, however, gives support for the conclusion that for experimental purposes the flap motion used yields a considerable improvement of the wave motion.

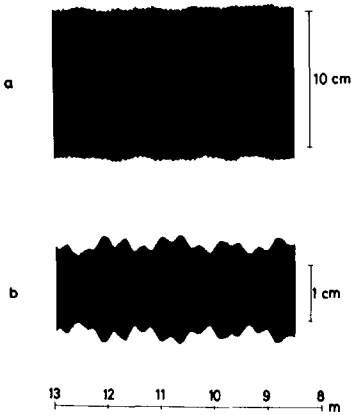


Fig. 15
Record of total wave motion and total second harmonic motion for non-sinusoidal flap motion

5. DISCUSSION OF OTHER PHENOMENA OBSERVED

In the experiments were observed or recorded some phenomena, other than the main object of the study.

The most obvious is the attenuation of the waves down the flume. In terms of wave heights the measured values for $\Delta H/H$ ranged between 0.002 per m for the longest waves and 0.006 - 0.013 per m for h/L about 0.5. Hence the total reduction in wave height over the 17 m test section was in some cases 20% corresponding to 36% of the energy at the wave generator being dissipated.

As all boundary layers are laminar the relative attenuation should be linear and independent of the wave steepness, which is confirmed by the measurements. Assuming boundary layers at the bottom and side walls yield $\Delta H/H$ values up to 0.0035. If in addition a boundary layer at the free surface is included, corresponding to a flexible film there (Van Dorn (1966)) the theoretical attenuation will exceed all measured values of $\Delta H/H$, being 0.022 for $h/L \sim 0.5$.

Another phenomenon is caused by resonant interaction between the waves present in the flume. This occurs when $\Delta k = k_{22} - 2k$ is small, i.e. for h/L small. The phenomenon was reported by Goda (1967) who found a variation with x of not only the amplitudes of the second and higher harmonic wave components. Also the first harmonic component showed a periodic amplitude variation with x , indicating slow-rate exchange of energy between the wave components. Mei and ŪnlŪata (1972) studied the problem analytically on the basis of the non-linear long wave equations and found good agreement with Goda's results.

Fig. 16 shows a record for $h/L = 0.095$ which clearly exhibits the same effects. Part a is the total wave motion, part b the first harmonic component, and part c the total second harmonic motion. (There

is a certain amount of first order reflection, which was later removed by introduction of the beach shown in Fig. 4.)

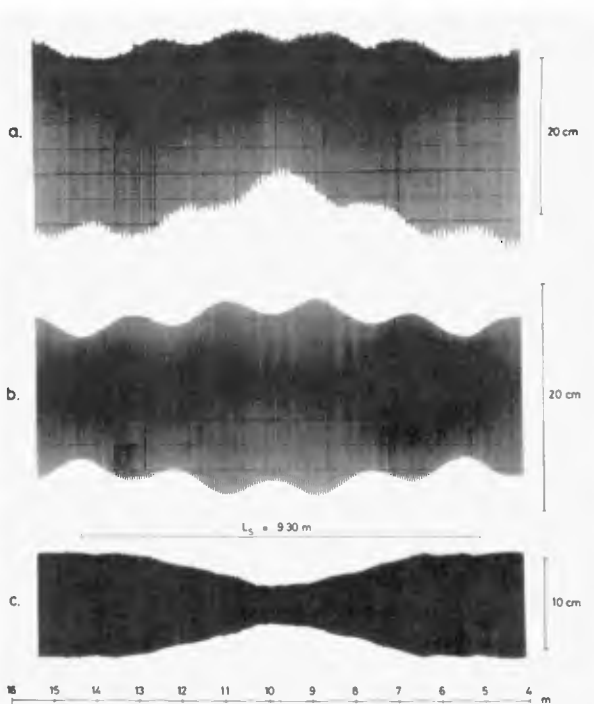


Fig. 16 Wave record with resonant interaction
($T = 2.3$ s, $h = 43$ cm, $\bar{H} = 21$ cm)

The phenomenon has not been studied explicitly in the experiments reported herein. However, it may be worth-while to mention that the resonant interaction in Fig. 16 at $h/L = 0.095$ ($kh = 0.60$) could not have been predicted by Mei and Ünlüata's analysis. Actually their theory is not valid at all for so large h/L , which is obvious, considering the fact that included in the phenomenon is a free second harmonic wave with frequency 2ω which corresponds to $h/L = 0.19$ (linear shallow water theory) or $h/L \sim 0.22$ (Stokes). The non-linear dispersion relation

$$\frac{\omega}{\sqrt{g/h}} = kh \left(1 - \frac{1}{6}(kh)^2\right) \quad (5-1)$$

used by Mei and Ünlüata yields no solution at all for k_{22} in the present case. This is illustrated in Fig. 17. The criterion for the occurrence of resonant interaction is $\Delta k/k \ll 1$. Therefore as Fig. 17 shows the resonant interaction must vanish when h/L becomes more than 0.12 - 0.14 (provided (1-2) is the proper dispersion relation). This is confirmed by the experimental results.

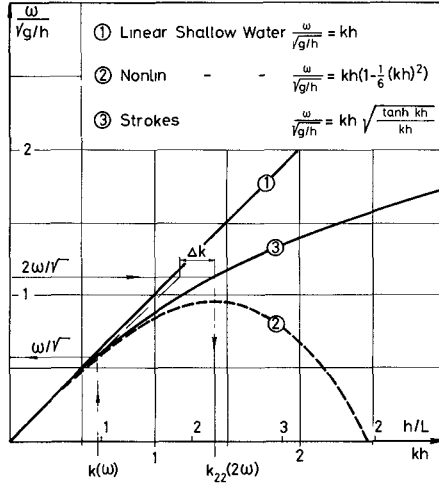


Fig. 17 Dispersion relations

A third irregularity which is observed for the shorter waves with 5 - 7% steepness, is shown in Fig. 18. The record represents the time variation at a fixed point after the start of the wave generator. Obviously, after some time the waves separate into groups with a beat amplitude which appears to depend strongly on the wave steepness. The pattern resembles the instability analysed by Benjamin and Feir (1967) although the beat length does not agree very well with their disturbance of maximum amplification. The phenomenon did not influence the measurements of L_s and H_{22} as it only occurred at the end of the flume for the wave heights and periods in question.

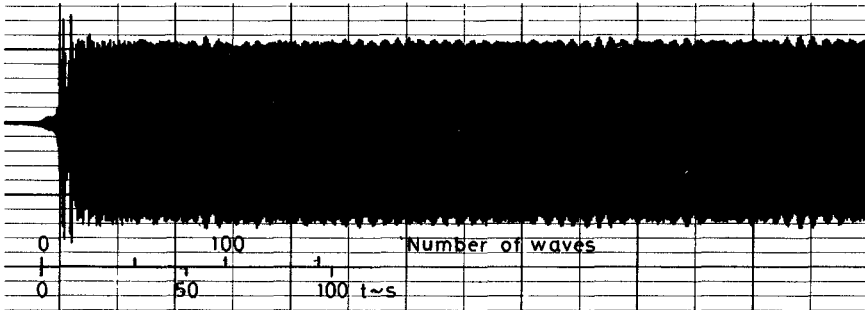


Fig. 18 Instability of waves at the end of the flume
($H = 3.8$ cm, $T = 0.65$ s, $h = 30$ cm)

Finally should be mentioned the second harmonic reflection which has already been shown in Fig. 15, part b. The frequency of the wave reflected is 2ω and the reflection was largest for waves of 2 - 2.5% steepness (more than 10% of H_2) and independent of the water depth. It is

likely that it is generated by the breaking process — the characteristics of which depends on the wave steepness.

6. SUMMARY AND CONCLUSION

The results from measurements on waves produced by sinusoidal piston motion of a flap type wave generator show that in the region tested, i.e. $0.10 < h/L < 0.65$, the wave motion in the flume is well described by (1-1). That is by a second order Stokes wave superimposed by a small free second harmonic wave with half the period of the main wave. This model ignores all higher order effects.

In the experiments were measured the total wave motion, and the first and second harmonic components. In Section 2 are described details of the experiments and the technique used for analysing data.

Results for the height of the free second harmonic wave component are shown in Fig. 6, and for its phase velocity in Fig. 9. All these results were obtained by sinusoidal piston motion of the flap.

In Fig. 11 some results are presented for the influence of an additional rotation of the flap.

Finally, in Section 4 are given results for a non-sinusoidal piston motion of the wave generator. The phase angle and amplitude of the second harmonic component of the flap motion were designed to minimize the free second harmonic wave.

In general it is found that the reproducibility of the measurements improves with increasing wave steepness, and apart from a series of unwanted side-effects (Section 5) which do not affect the measurements the results seem to be consistent.

This is also confirmed by the conclusion that the non-sinusoidal flap motion of Section 4 yields a wave motion in the flume which for almost all practical purposes may be said to represent a wave of constant form.

7. REFERENCES

1. Benjamin, T.B., and Feir, J.E., 'The Disintegration of Wave Trains on Deep Water,' Part 1, Jour. Fluid Mech., Vol. 27, 3, 1967, pp. 417-430.
2. Biéssel, F., and Suquet, F., 'Les Appareils Générateurs de Houle en Laboratoire,' La Houille Blanche, Vol. 6, Nos. 2, 4 and 5, 1951.
3. Brink-Kjær, O., 'Amplitude Dispersive Waves. A Comparison Between Phase Velocities,' Prog. Rep. 33, Inst. Hydrodyn. and Hydraulic Engrg., Tech. Univ. Denmark, 1974, pp. 27-33.
4. Daugaard, E., 'Generation of Regular Waves in the Laboratory,' Unpubl. thesis (in Danish), Inst. Hydrodyn. and Hydraulic Engrg., Tech. Univ. Denmark, 1972.
5. Fontanet, P., 'Theorie de la Génération de la Houle Cylindrique par un Batteur Plan,' La Houille Blanche, Vol. 16, Nos. 1-2, 1961.

6. Goda, Y., 'Travelling Secondary Wave Crests in Wave Channels,' Appendix to Rep. No. 13, Port and Harbour Res. Inst., Ministry Transp., Japan, 1967.
7. Hulsbergen, C.H., 'Golfopwekking in Relatief Ondiep Water,' Waterloopkundig Laboratorium, Delft, 1972.
8. Iwagaki, Y., and Sakai, T., 'Horizontal Water Particle Velocity of Finite Amplitude Waves,' Proc. 12th Conf. Coastal Engrg., Vol. 1, 1970, pp. 309-325.
9. Le Méhauté, B., Divoky, D., and Lin, A., 'Shallow Water Waves: A Comparison of Theories and Experiments,' Proc. 11th Conf. Coastal Engrg., 1968, pp. 86-106.
10. Madsen, O.S., 'Waves Generated by a Piston-Type Wavemaker,' Proc. 12th Conf. Coastal Engrg., 1970, pp. 589-607.
11. Madsen, O.S., 'On the Generation of Long Waves,' Jour. Geophys. Res., Vol. 36, 1971, pp. 8672-8683.
12. Madsen, O.S., Mei, C.C., and Savage, R.P., 'The Evolution of Time-Periodic Long Waves of Finite Amplitude,' Jour. Fluid Mech., Vol. 44, 1, 1970, pp. 195-208.
13. Mei, C.C., and Ūnlūata, Ū., 'Harmonic Generation in Shallow Water Waves,' in 'Waves on Beaches,' R.E. Meyer, ed., 1972, pp. 181-202.
14. Morison, J.R., and Crooke, R.C., 'The Mechanics of Deep Water, Shallow Water and Breaking Waves,' Tech. Memo No. 40, Beach Erosion Board, 1953.
15. Sørensen, P.S., and Schiøltzen, P., 'Digital Control of Hydraulic Generators,' Unpubl. thesis (in Danish), Inst. Circuit Theory and Telecommunication, and Inst. Hydrodyn. and Hydraulic Engrg., Tech. Univ. Denmark, 1973.
16. Van Dorn, W.G., 'Boundary Dissipation of Oscillatory Waves,' Jour. Fluid Mech., Vol. 24, 4, 1966, pp. 769-780, (Corrigendum, Jour. Fluid Mech., Vol. 32, 4, 1968, pp. 828-829).